

See discussions, stats, and author profiles for this publication at: <https://www.researchgate.net/publication/224281991>

# An experimental and theoretical study of molecular structure and vibrational spectra of 2-chloronicotinic acid by density functional theory and ab initio Hartree–Fock calculations

ARTICLE *in* JOURNAL OF MOLECULAR STRUCTURE · AUGUST 2008

Impact Factor: 1.6 · DOI: 10.1016/j.molstruc.2007.10.004

---

CITATIONS

63

---

READS

101

3 AUTHORS, INCLUDING:



Mehmet Karabacak

Celal Bayar Üniversitesi

131 PUBLICATIONS 1,481 CITATIONS

SEE PROFILE



Mustafa Kurt

Ahi Evran Üniversitesi

106 PUBLICATIONS 1,429 CITATIONS

SEE PROFILE

# An experimental and theoretical study of molecular structure and vibrational spectra of 2-chloronicotinic acid by density functional theory and ab initio Hartree–Fock calculations

Mehmet Karabacak<sup>a,\*</sup>, Mehmet Çınar<sup>a</sup>, Mustafa Kurt<sup>b</sup>

<sup>a</sup> *Department of Physics, Afyonkarahisar Kocatepe University, TR-03040, Afyonkarahisar, Turkey*

<sup>b</sup> *Department of Physics, Ahi Evran University, TR-40100, Kırşehir, Turkey*

Received 29 June 2007; received in revised form 3 October 2007; accepted 4 October 2007

Available online 12 October 2007

## Abstract

In this work, the Fourier transform Raman and Fourier transform infrared spectra of 2-chloronicotinic acid (2-CNA) are recorded in the solid phase. The molecular geometry, vibrational frequencies, infrared intensities and Raman scattering activities of 2-CNA in ground state have been calculated by using ab initio Hartree–Fock (HF) and density functional (B3LYP and B3PW91) methods with 6-31G(d) and 6-311G(d) basis sets level. On the basis of the comparison between calculated and experimental results and the comparison with related molecule, assignments of fundamental vibrational modes are examined. The optimized geometric parameters (bond lengths and bond angles) obtained by using HF show the best agreement with the experimental values of 2-CNA. Comparison of the observed fundamental vibrational frequencies of 2-CNA and calculated results by density functional (B3LYP and B3PW91) and Hartree–Fock methods indicates that B3LYP is superior to the scaled Hartree–Fock and B3PW91 approach for molecular vibrational problems.

© 2007 Elsevier B.V. All rights reserved.

**Keywords:** Infrared and Raman spectra; Ab initio calculations; HF; DFT; 2-Chloronicotinic acid; Vibrational frequencies

## 1. Introduction

Nicotinic acid, widely known as niacin, a compound of water-soluble vitamin B complex, is active in the metabolism of body, and is key ingredient in animal feed and animal feed premixes as this contributes to numerous metabolic reactions as hydrogen transferring coenzymes. It acts to reduce plasma cholesterol, as a vasodilator and to treat pellagra. Nicotinic acid and its derivatives, which have good biological activities and versatile bonding modes, have been studied extensively [1]. The structures of many of the complexes that have been reported show nicotinic acid and its derivatives acting as bridging ligands through the carboxylate group and pyridyl N atom [1]. The solid-state structure of nicotinic acid was first determined

in 1953 [2] and later revisited [3]. The nicotinic acid and its complexes with different metals were thoroughly investigated using different methods [4]. The biological importance of this type of compounds and especially its complexes are described in the literature [5,6]. 2-Chloronicotinic acid is important building block for agrochemicals, feed additives, animal food enrichment and pharmaceuticals [7].

Vibrational assignment based FT-IR and Raman spectra have been reported for nicotinic acid [5,6] but for 2-CNA molecule such experimental vibrational assignment has not been performed yet. Up to our knowledge, no detailed ab initio Hartree–Fock (HF) and density functional theory (DFT) calculations have been performed on 2-CNA, and analysis of the vibrational modes of this molecule using quantum chemical methods have not been published. Extensive experimental and theoretical investigations have focused on elucidating the structure and

\* Corresponding author. Tel.: +90 272 2281311; fax: +90 272 2281235.  
E-mail address: [karabacak@aku.edu.tr](mailto:karabacak@aku.edu.tr) (M. Karabacak).

normal vibrations of nicotinic acid derivatives. The aim of this study is to calculate optimal molecular geometry, vibrational frequencies and normal modes associated of free 2-CNA and to find effective methods that would offer a higher certainty of finding vibrational wavenumbers and molecular parameters.

The calculated harmonic frequencies are usually higher than the corresponding experimental quantities, due to a combination of electron correlation effects and basis set deficiencies. It is well known that HF method tends to overestimate vibrational frequencies. However, DFT calculations are reported to provide excellent vibrational frequencies of organic compounds if the calculated frequencies are scaled to compensate for the approximate treatment of electron correlation for basis set deficiencies and the anharmonicity [8–14].

Based on experimental data of 20 small organic molecules, Rauhut and Pulay have shown that B3LYP

method leads to geometry parameters close to experimental data [14]. Therefore, we expect that B3LYP calculated geometry of studied molecule is in good agreement with their experimental geometric parameters. As seen in Tables 1 and 2, our calculated results indicate that the aromatic ring of 2-CNA molecule is distorted from regular hexagon due to steric and electronic effects of carboxylic acid and chlorine substituent of the nicotinic acid.

In this study, geometric parameters, the IR and Raman spectra 2-CNA in the ground state were examined for the first time by using the Gaussian 03 suite of quantum chemical codes [15]. A detailed quantum chemical study will aid in making definite assignments to the fundamental normal modes of 2-CNA and in clarifying the experimental data available for this important molecule. Ab initio HF and DFT calculations have been performed to support our vibrational assignments.

Table 1  
Geometric parameters, bond lengths (Å) and bond angles (°), optimized for 2-CNA

Parameters	X-ray <sup>a</sup>	6-31G(d)			6-311G(d)		
		HF	B3LYP	B3PW91	HF	B3LYP	B3PW91
<i>Bond lengths</i>							
C(1)–C(2)	1.394	1.401	1.414	1.411	1.401	1.411	1.409
C(1)–Cl(10)	1.730	1.730	1.750	1.737	1.731	1.751	1.736
C(1)–N(14)	1.320	1.307	1.324	1.322	1.305	1.320	1.318
C(2)–C(3)	1.396	1.391	1.404	1.401	1.391	1.401	1.399
C(2)–C(9)	1.505	1.493	1.493	1.490	1.493	1.493	1.490
C(3)–C(4)	1.382	1.381	1.390	1.388	1.380	1.387	1.385
C(3)–H(6)	0.950	1.072	1.083	1.084	1.071	1.082	1.083
C(4)–C(5)	1.387	1.380	1.393	1.391	1.379	1.390	1.388
C(4)–H(7)	0.950	1.073	1.085	1.085	1.073	1.084	1.084
C(5)–H(8)	0.950	1.075	1.088	1.089	1.075	1.087	1.087
C(5)–N(14)	1.349	1.321	1.337	1.334	1.320	1.334	1.331
C(9)–O(11)	1.201	1.185	1.210	1.208	1.179	1.203	1.202
C(9)–O(12)	1.328	1.334	1.363	1.357	1.332	1.361	1.355
O(12)–H(13)	0.840	0.952	0.975	0.973	0.944	0.969	0.967
$\sigma$ (RMS)		0.065	0.065	0.073	0.064	0.072	0.072
<i>Bond angles</i>							
C(2)–C(1)–Cl(10)	122.2	122.4	122.1	122.0	122.5	122.1	122.0
C(2)–C(1)–N(14)	123.9	123.4	123.7	123.7	123.5	123.7	123.7
Cl(10)–C(1)–N(14)	113.8	114.2	114.2	114.3	114.0	114.2	114.3
C(1)–C(2)–C(3)	116.1	116.5	116.3	116.3	116.3	116.2	116.2
C(1)–C(2)–C(9)	124.3	124.4	124.3	124.2	124.5	124.4	124.4
C(3)–C(2)–C(9)	119.6	119.2	119.5	119.4	119.2	119.4	119.4
C(2)–C(3)–C(4)	120.8	120.4	120.4	120.4	120.4	120.4	120.5
C(2)–C(3)–H(6)	119.6	119.2	118.8	118.8	119.1	118.8	118.8
C(4)–C(3)–H(6)	119.6	120.4	120.8	120.8	120.4	120.8	120.8
C(3)–C(4)–C(5)	118.4	117.5	117.8	117.7	117.4	117.8	117.7
C(3)–C(4)–H(7)	120.8	121.5	121.3	121.3	121.5	121.3	121.3
C(5)–C(4)–H(7)	120.8	121.1	120.9	121.0	121.1	120.9	121.0
C(4)–C(5)–H(8)	119.3	121.0	121.1	121.1	121.1	121.3	121.2
C(4)–C(5)–N(14)	121.5	123.3	123.2	123.3	123.3	123.1	123.2
H(8)–C(5)–N(14)	119.3	115.7	115.7	115.6	115.6	115.7	115.6
C(2)–C(9)–O(11)	124.6	126.7	127.0	126.9	127.0	127.1	127.0
C(2)–C(9)–O(12)	111.9	111.6	111.4	111.3	111.5	111.3	111.3
O(11)–C(9)–O(12)	123.5	121.7	121.6	121.8	121.5	121.6	121.7
C(9)–O(12)–H(13)	109.5	107.5	105.2	105.2	108.2	106.3	106.2
C(1)–N(14)–C(5)	119.2	119.1	118.6	118.6	119.1	118.8	118.7
$\sigma$ (RMS)		1.306	1.582	1.588	1.307	1.476	1.497

<sup>a</sup> The X-ray data from Ref. [16].

Table 2  
Comparison of the calculated and experimental (FT-IR and Raman) vibrational spectra of free 2-CNA

Normal mode	HF/6-31G(d)			B3LYP/6-31G(d)			B3PW91/6-31G(d)			HF/6-311G(d)			B3LYP/6-311G(d)			B3PW91/6-311G(d)			Experimental in this study	Approximate assignments*
	Freq <sup>a</sup>	I(IR)	I(R)	Freq <sup>b</sup>	I(IR)	I(R)	Freq <sup>c</sup>	I(IR)	I(R)	Freq <sup>d</sup>	I(IR)	I(R)	Freq <sup>e</sup>	I(IR)	I(R)	Freq <sup>f</sup>	I(IR)	I(R)		
<i>A'</i>																				
1	191	0.4	0.5	194	0.4	0.7	191	0.4	0.6	199	0.5	0.4	197	0.4	0.6	196	0.5	0.5	330(371)	i.p. COOH+ring bending
2	296	0.4	1.1	297	0.5	1.6	295	0.6	1.6	299	0.4	1.2	298	0.7	1.6	298	0.7	1.6		i.p. COOH+ring def.+C–Cl str.
3	350	3.0	3.5	350	2.3	3.5	349	2.1	3.5	355	2.7	3.6	351	2.3	3.6	352	2.1	3.5		i.p. COOH+ring def.+C–Cl bending
4	444	3.5	8.3	440	4.9	8.4	443	4.5	7.9	447	2.6	7.8	441	4.6	8.7	445	4.0	8.0	503	o.o.p. CCH+NCH+OH bending CCH bending
5	518	12.4	2.5	507	11.7	3.1	507	11.0	3.0	513	14.0	3.5	504	14.6	3.5	504	13.4	3.6		i.p. C=O bending+C–Cl str.+CCH bending
6	620	23.2	1.7	616	21.3	0.4	611	22.6	0.6	630	21.4	1.8	623	19.4	0.4	619	19.7	0.5	654(672)	i.p. ring def.
7	678	80.4	10.2	670	60.4	10.5	669	63.1	10.1	687	87.2	10.3	674	65.2	10.7	675	68.1	10.5		i.p. sym. C–O def.+C-Cl str.+ring def.
8	791	25.7	1.7	784	27.1	2.6	783	27.3	2.7	799	26.9	2.1	786	30.5	3.1	787	29.6	3.2		821
9	1038	58.0	7.5	1022	127.4	2.0	1021	116.0	1.8	1045	19.5	17.6	1022	150.0	2.0	1025	133.8	1.6	1058	CCH bending+CNC bending+CCH bending
10	1047	58.1	23.2	1050	25.2	30.4	1048	19.7	29.4	1055	109.2	17.6	1048	34.6	34.3	1050	26.3	33.0	1059	Ring breathing+C–OH str.
11	1073	49.6	13.7	1107	98.8	0.8	1112	102.2	1.2	1071	52.5	14.5	1101	92.9	0.9	1111	97.0	1.6	1068(1062)	C–OH str.+CH bending+CCN+CCC bending
12	1133	48.0	1.7	1125	47.1	3.5	1119	34.8	3.4	1138	43.5	2.3	1123	53.0	3.3	1122	39.1	3.0	1133(1133)	i.p. C–H bending
13	1157	3.6	2.6	1168	165.6	24.4	1165	173.8	24.6	1164	3.8	1.9	1169	178.5	25.6	1171	198.0	26.0	1149(1160)	i.p. OH bending+C–COOH str.+CH bending
14	1195	262.6	14.7	1236	7.1	3.2	1230	8.6	2.4	1211	303.0	16.4	1233	4.6	4.9	1233	8.3	2.1	1230(1233)	CCH bending+C–C+CN str.
15	1242	5.5	1.5	1266	4.5	9.9	1282	1.0	10.3	1252	7.1	1.0	1251	12.4	8.4	1273	4.1	11.2	1261	i.p. C–H bending
16	1339	104.6	3.9	1326	70.7	6.9	1326	86.3	7.2	1349	73.5	3.1	1323	46.7	4.4	1326	62.6	5.2	1406	CCH bending+C–C+CN str.+OH bending
17	1416	164.7	1.7	1399	126.9	3.7	1397	127.8	3.8	1423	175.8	1.4	1393	137.0	2.9	1397	136.4	3.0		CCH bending+C–C+CN str.+OH bending
18	1445	6.1	1.0	1432	2.2	3.2	1425	5.3	3.7	1455	4.9	1.0	1429	1.5	3.6	1427	4.6	3.8		1452
19	1579	111.9	16.6	1549	63.9	18.4	1551	67.4	18.1	1590	116.8	17.6	1543	63.7	18.5	1552	69.0	18.5	(1569)	C–C+C–N str.
20	1603	117.1	40.4	1578	79.4	40.0	1581	82.6	38.5	1612	126.2	43.4	1572	85.6	40.4	1581	88.7	39.2	1581(1584)	C–C+C–N str.
21	1819	456.3	23.0	1771	269.9	45.5	1776	275.3	44.6	1827	493.3	24.0	1762	300.3	46.1	1773	306.3	46.1	1721(1712)	C=O str
22	3021	12.1	87.7	3071	15.6	120.2	3059	15.5	121.4	3037	13.9	88.4	3060	16.3	121.5	3057	16.2	118.8	3063(3065)	C–H str
23	3041	15.2	136.7	3103	10.6	143.5	3093	8.3	130.5	3059	19.0	145.1	3092	14.1	158.5	3092	11.3	142.4	3074(3077)	C–H str
24	3064	1.9	99.9	3127	1.3	98.8	3113	1.7	107.9	3090	1.9	89.6	3121	1.5	97.4	3117	1.7	100.2	3097(3098)	C–H str
25	3623	164.3	99.1	3564	82.0	147.7	3572	91.7	144.0	3736	131.2	97.6	3620	67.8	150.0	3632	73.1	142.3		O–H str
<i>A''</i>																				
1	25	0.7	0.2	14	0.4	0.2	18	0.5	0.2	7	0.6	0.0	14	0.4	0.0	11	0.4	0.0	12	COOH+Ring torsion
2	110	0.8	2.8	103	0.7	2.4	102	0.6	2.4	111	0.7	2.1	102	0.6	1.9	100	0.6	1.9	(143)	o.o.p. ring+COOH bending+C–Cl bending
3	214	2.4	1.9	211	1.7	1.6	208	2.2	1.7	220	3.1	1.3	212	2.8	1.1	212	3.2	1.1	(240)	o.o.p. ring+COOH bending
4	420	0.6	1.0	417	0.4	1.7	411	0.5	1.5	432	1.4	0.8	422	0.9	1.4	418	1.0	1.2		o.o.p. CCH+NCH+OH bending
5	494	2.8	0.8	486	1.9	0.6	482	2.0	0.6	506	1.3	0.2	492	1.5	0.2	490	1.9	0.2	(460)	o.o.p. CCC bending+C–OH bending+C–Cl str.
6	571	128.0	4.0	591	98.9	6.5	591	99.2	5.9	586	138.9	4.5	600	108.7	6.7	602	109.1	6.1	540(545)	o.o.p. OH bending
7	727	5.4	0.3	709	15.9	0.4	708	15.2	0.4	739	4.6	0.3	719	16.3	0.5	720	16.2	0.5	716(716)	o.o.p. CCH+CCC,CCN bending+C–COOH bending
8	773	101.3	2.6	749	54.6	2.8	746	62.6	2.7	785	109.5	1.4	758	69.2	2.0	757	73.6	1.6	771	o.o.p. CCH+CCC+CCN bending+C–COOH bending
9	830	1.0	0.4	807	3.0	0.9	802	2.9	0.6	844	1.0	1.3	817	1.1	0.3	816	0.6	0.4	834(828)	o.o.p. C–H+CCC+O–H bending
10	995	0.3	1.5	947	0.1	2.3	941	0.1	2.1	1006	0.0	0.4	951	0.0	0.6	948	0.0	0.5	972	o.o.p. C–H bending
11	1011	0.4	0.4	965	0.6	0.2	959	0.7	0.2	1020	0.0	0.3	973	0.3	0.1	969	0.3	0.1	985	o.o.p. C–H bending
$\sigma$	28,965			24,508			25,787			29,649			22,984			24,692				

Raman values are given in parentheses [Frequency (cm<sup>-1</sup>), IR intensities (km mol<sup>-1</sup>), Raman scattering activities (Å amu<sup>-1</sup>)].

<sup>a</sup> Scaling factor (s.f.): 0.8929.

<sup>b</sup> s.f.: 0.963.

<sup>c</sup> s.f.: 0.9567.

<sup>d</sup> s.f.: 0.9044.

<sup>e</sup> s.f.: 0.9663.

<sup>f</sup> s.f.: 0.9627.

\* str.: stretching, i.p.: in plane, o.o.p.: out-of-plane.

## 2. Experimental

The compound 2-chloronicotinic acid in solid state was purchased from Acros Organics Company with a stated purity of 99% and it was used as such without further purification. The sample was prepared using a KBr disc technique. The infrared spectrum of compound was recorded between  $4000\text{ cm}^{-1}$  and  $400\text{ cm}^{-1}$  on a Perkin-Elmer FT-IR System Spectrum BX spectrometer which was calibrated using polystyrene bands and under  $400\text{ cm}^{-1}$  on Bruker IFS 66/S. The Raman spectrum of compounds was recorded between  $3500\text{ cm}^{-1}$  and  $5\text{ cm}^{-1}$  on FRA 106/S spectrometer.

## 3. Computational details

Geometry optimization was started from the X-ray experimental atomic positions [16]. The molecular structure of 2-CNA in the ground state (in vacuo) is optimized by HF, B3LYP and B3PW91 with the 6-31G(d) and 6-311G(d) basis sets level. The optimized structural parameters were used in the vibrational frequency calculations at the HF and DFT levels.

Density functional theory for all studies reported in this paper has the following form:

$$E_{\text{XC}} = (1 - a_0)E_{\text{X}}^{\text{LSDA}} + a_0E_{\text{X}}^{\text{HF}} + a_{\text{X}}\Delta E_{\text{X}}^{\text{B88}} + a_{\text{C}}E_{\text{C}}^{\text{LYP}} + (1 - a_{\text{C}})E_{\text{C}}^{\text{VWN}}$$

where the energy terms are the Slater exchange, the Hartree–Fock exchange, Becke's exchange functional correction, the gradient corrected correlation functional of Lee, Yang and Parr, and the local correlation functional of Vosko et al. [17]. HF, B3LYP and B3PW91 with the 6-31G(d) and 6-311G(d) basis set levels of theory with optimized geometry has been used to calculate all parameters of 2-CNA molecule. Default optimization specifications were normally used. If symmetry constrains led to a transition state or hilltop, instead of a minimum, this would show up as the presence of one or more imaginary frequencies not belonging to the totally symmetric irreducible representation.

All the calculated vibrational frequencies are scaled by 0.8929 [18], 0.9044 for HF, 0.963, 0.9663 for B3LYP and 0.9567, 0.9627 for B3PW91 for 6-31G(d) and 6-311G(d) basis sets, respectively [19]. Molecular geometry is not restricted and all the calculations (vibrational wavenumbers, geometric parameters and other molecular properties) are performed by using GaussView molecular visualisation program [20] and GAUSSIAN 03-program package on the personal computer [15].

By combining the results of the GaussView program [20] with symmetry considerations, vibrational frequency assignments were made with a high degree of accuracy. There is always some ambiguity in defining internal coordinates. However, the defined coordinate form complete set

and matches quite well with the motions observed using the GaussView program [21].

## 4. Results and discussion

The molecule of 2-CNA consists of 14 atoms, so it has 36 normal vibrational modes. On the assumption of a  $C_s$  symmetry the numbers of vibration modes of the 36 fundamental vibrations of 2-CNA molecule ( $N=14$ ) are  $25A' + 11A''$ . The vibrations of the  $A'$  species are in plane and those of the  $A''$  species are out of plane. All the 36 fundamental vibrations are active in both IR and Raman. But if the molecule was  $C_1$  point group there would not be any relevant distribution.

Optimized ground-state geometries and vibrational modes for studied molecular structures were obtained by ab initio HF and DFT (B3LYP and B3PW91) with the 6-31G(d) and 6-311G(d) levels and compared with the experimental crystal geometry (bond lengths and bond angles) and experimental frequencies. Souza et al. [16] have reported on molecular structure (bond lengths and bond angles) of 2-CNA by X-ray diffraction methods.

### 4.1. Molecular geometries

The first task for the computational work was to determine the optimized geometry of 2-CNA. The theoretical and experimental crystal structure of the (2-CNA) compound was shown in Fig. 1. The numbering of the atoms of 2-CNA is shown in Fig. 1(a). The geometric structure of the compound is orthorhombic with space group  $Pna2_1$  and the cell dimensions  $a = 8.2741(2)\text{ \AA}$ ,  $b = 13.1807(5)\text{ \AA}$ ,  $c = 5.7182(3)\text{ \AA}$  and  $V = 623.62(4)\text{ \AA}^3$  [16]. The optimized structure parameters (bond lengths and bond angles) of 2-CNA calculated ab initio HF and DFT (B3LYP and B3PW91) with the 6-31G(d) and 6-311G(d) basis set listed in Table 1 in accordance with the atom numbering scheme given in Fig. 1(a). In the second column of Table 1, the available experimental data obtained by the X-ray study for 2-CNA [16] is also included.

The optimized parameters obtained by the HF, B3LYP and B3PW91 methods are approximately similar. It is well known that HF method under estimate some bond lengths [22]. As seen from Table 1 the CN distances are calculated at the HF level of theory with a value smaller than the experimental value, comparing with the B3LYP and B3PW91 level of theory. Using these methods similar calculations were found for pyridine [23], methyl pyridine [24], phthalazine [25] and 2-chlorolepidine [26].

Taking into account that the molecular geometry in the vapour phase may be different from in the solid phase, owing to extended hydrogen bonding and stacking interactions there is reasonable agreement between the calculated and experimental geometric parameters. As discussed by

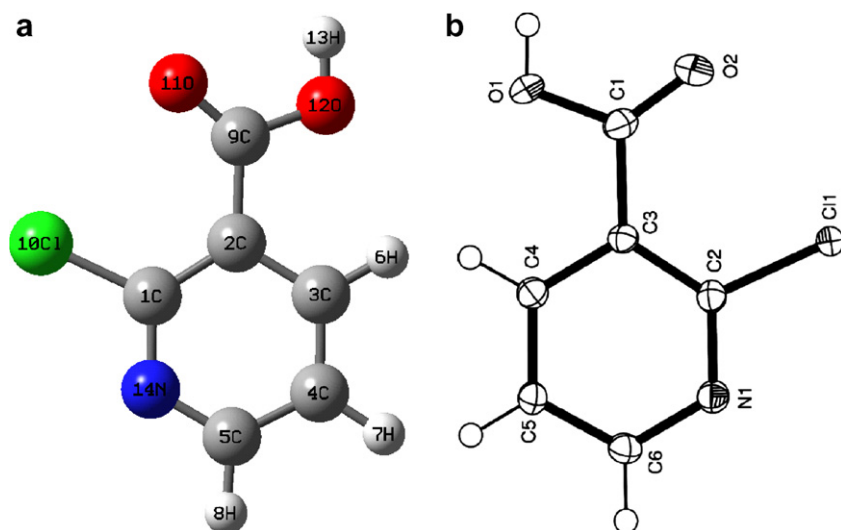


Fig. 1. (a) The theoretical geometric structure and atoms numbering of the title compound (2-CNA). (b) The experimental geometric structure of the title compound (2-CNA) (displacement ellipsoids and H atoms shown as small circles of arbitrary radii are drawn at the 50% probability level) taken from Ref. [16].

Johnson et al. [27], DFT method predicts bond lengths which are systematically too long, particularly the CH bond lengths. This theoretical pattern also is found for 2-CNA, since the large deviation from experimental CH bond lengths may arise from the low scattering of hydrogen atoms in the X-ray diffraction experiment. For example, CH bond lengths values in the experiment are 0.95 Å but the values in the theoretical result are bigger than 1 Å.

The experimental bond length CCl is 1.730 Å for 2-CNA. Our calculated values change from 1.730 Å to 1.751 Å for all methods which are in good agreement with in crystal structure of 2-CNA molecule [16]. The experimental bond length value is equal to the theoretical value by using HF method. Bakiler et al. calculated this bond length as 1.746 Å for 3-chloropyridine [28] and 1.748 Å for 2-chloropyridine [29] by using force field calculations. These bond lengths were also observed in 1.735–1.744 Å range for similar molecules [30,31].

The optimized bond angles of C–C–C and C–N–C in pyridine ring fall in the range from 116° to 119°, except C2–C3–C4 (120.8°) for 2-CNA, which are smaller hexagonal angle of 120° for studied molecule. But C–C–N angles are found to be bigger than approximately 4° hexagonal angles. Similar values are found for other pyridine derivatives [30–32].

To make comparison with experimental data, we present RMS ( $\sigma$ ) values based on the calculations bottom of Table 1. As seen in table the bond lengths and bond angles calculated by means of the HF method are the closest to experimental data and HF method correlates well for bond lengths and bond angles compared with other methods. The best RMS bond lengths value is about 0.064 for HF/6-311G(d) level of theory, and bond angle values are also about 1.306 and 1.307 for the HF method with 6-31G(d) and 6-311G(d) for the studied molecule.

#### 4.2. Vibrational spectra

The experimental IR and Raman spectra of 2-CNA are given in Fig. 2. The theoretical vibrational spectra of this molecule was calculated by using ab initio HF and DFT (B3LYP and B3PW91) with the 6-31G(d) and 6-311G(d) basis set. The simulated infrared and Raman spectra are shown in Fig. 3, where the calculated intensity is plotted against the vibrational frequencies. The resulting vibrational frequencies for the optimized geometries and the proposed vibrational assignments as well as IR intensities and Raman scattering activities are given in Table 2. The proposed vibrational assignments are given in the last column of Table 2. The high degree of symmetry of the molecules is also helpful in making vibrational assignments. They are made by inspection of each of the vibrational mode at HF/6-31G(d) level. Modes are numbered from smallest to largest frequency.

The comparisons of theoretical and experimental IR spectra indicate that the intense vibrations in the experimental spectrum are also intense in theoretical spectrum. The calculated vibrational wavenumbers using different methods were compared with the experimentally observed values. Some bands found in the predicted IR spectra were not observed in the experimental spectrum of 2-CNA. For example, hydrogen bonding in the condensed phase with the other acid molecules makes vibrational spectra more complicated. Therefore we could not observe the strong and sharp bands of O–H vibration in the IR and Raman spectra.

As seen in Table 2, there is great mixing of the ring vibrational modes and also between the ring and substituent modes. The descriptions of the modes are very complex because of the low symmetry of the studied molecule. Especially, the out of plane modes are the most difficult to be



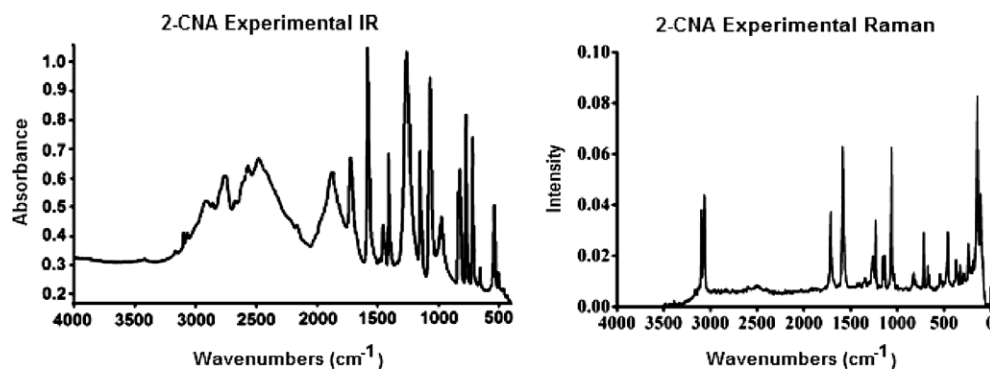


Fig. 2. Experimental IR and Raman spectra of 2-CNA molecule.

assigned due to mixing with the ring modes and also with the substituent modes. There are some strong frequencies useful to characterize in the IR and Raman spectrum.

For 2-CNA group the vibrational modes are C–H stretch, C–O stretch, C–Cl stretch, C–N stretch, O–H stretch, C–C–H bending, C–C–C bending, C–C–N bending, ring bending and ring torsion. As seen from Table 2, in general the C–H vibration frequencies calculated theoretically are in good agreement with experimentally reported values for 2-CNA. The vibrational modes due to the CH stretching are generally observed between 3000  $\text{cm}^{-1}$  and 3100  $\text{cm}^{-1}$  experimentally, which are 3063(IR), 3065(R), 3074(IR), 3077(R), 3097(IR) and 3098(R) for 2-CNA. There are also three calculated values that correspond to symmetric and asymmetric CH stretching vibrations of the same region. In the high frequency region, calculated B3LYP values are more reliable than HF values.

Some vibrational modes were shown to be Cl-sensitive modes whereas others were calculated in a narrow frequency range. The theoretical wavenumbers of C–Cl stretching vibration are coupled with other group vibrations. Ring–Cl modes are partially C–Cl stretching and bending modes have been reported to a frequency range of 200–800  $\text{cm}^{-1}$ . The ring halogen stretching mode was observed as weak to medium IR bands at 330 and 503  $\text{cm}^{-1}$  for chlorine. The bending modes were located at 280,300  $\text{cm}^{-1}$  range for chloro derivatives. The calculated bending mode is approximately 349–355  $\text{cm}^{-1}$  and 100–110  $\text{cm}^{-1}$  range for 2-CNA by using all methods (see Table 2) however, the observed as strong Raman bands (143  $\text{cm}^{-1}$ ) should be lattice mod because our molecule is in solid state. Other  $\nu(\text{C–Cl})$  character involving modes are 492, 504 and 674  $\text{cm}^{-1}$  using B3LYP. In the earlier vibrational studies of 3-chloro-2-, 2-chloro-6-, 4-chloro-2- and 5-chloro-2-methyl anilines are observed 650–670  $\text{cm}^{-1}$  the  $\nu(\text{C–Cl})$  bands [30,33,34]. The theoretical wavenumbers of C–Cl stretching vibration are coupled with other group vibrations.

O–H stretching band is characterized by very broad-band appearing near about 2500–3600  $\text{cm}^{-1}$ . This may be combined effect of intermolecular hydrogen bonding. The O–H in plane bending vibration occurs in the general of

1440–1395  $\text{cm}^{-1}$ . The O–H out of plane bending vibration occurs in 960–875  $\text{cm}^{-1}$  [21]. In 2-CNA, O–H in plane bending and out of plane bending vibrations are assigned to 1406 and 834(828)  $\text{cm}^{-1}$ , respectively. Theoretically computed values (1393 and 830  $\text{cm}^{-1}$ ) are in very good agreement with experimental results.

The most characteristic feature of carboxylic group is a single band observed usually in the 1700–1800  $\text{cm}^{-1}$  region. This band is due to the C=O stretching vibration. Intense band assigned to stretching vibrations  $\nu(\text{C=O})$  1721  $\text{cm}^{-1}$  (IR) and 1712  $\text{cm}^{-1}$  (R) for title compound. For nicotinic acid, picolinic acid and isonicotinic acid this band occurs at 1708, 1717 and 1712  $\text{cm}^{-1}$ , respectively [5]. It means that presence of nitrogen in aromatic ring and its position versus carboxylic acid influence the mode form very slightly, but in the experimental spectra the shift of various bands along with the change of nitrogen position is remarkable. By the chlorine substitution in place of hydrogen atom, the chlorine position versus carboxylic anion influence the C=O mode form remarkably but this is not true for C=C bands. The theoretically computed value of C=O bands show very good agreement with experimental results, especially for B3LYP method. The HF methods gave a higher  $\nu(\text{C=O})$  than the other methods. All present assignments agree well with the values available in the literature [5,6,21,26,28–30,33,34].

The C–C vibrations calculated at 1578 and 1581  $\text{cm}^{-1}$  (using B3LYP and B3PW91) are in excellent agreement with experimental observations of 1581  $\text{cm}^{-1}$  in FTIR spectrum. The theoretically calculated C–C–C out of plane and in plane bending modes have been found consistent with the recorded spectral values.

Infrared intensities for 2-CNA from experimental fundamentals at 1581  $\text{cm}^{-1}$  are very strong, theoretical intensities of these fundamentals are not in the same order. This mode corresponds to C–C stretching. The most intense Raman peak is calculated to be at 3041, 3103 and 3093  $\text{cm}^{-1}$  (HF, B3LYP and B3PW91, respectively) using 6-31G(d) and 3059, 3092 and 3092  $\text{cm}^{-1}$  (HF, B3LYP and B3PW91, respectively) 6-311G(d), and corresponds to the in plane pyridine ring C–H stretching.

In general, our infrared and Raman intensities are very high when compared with those at the lower frequency

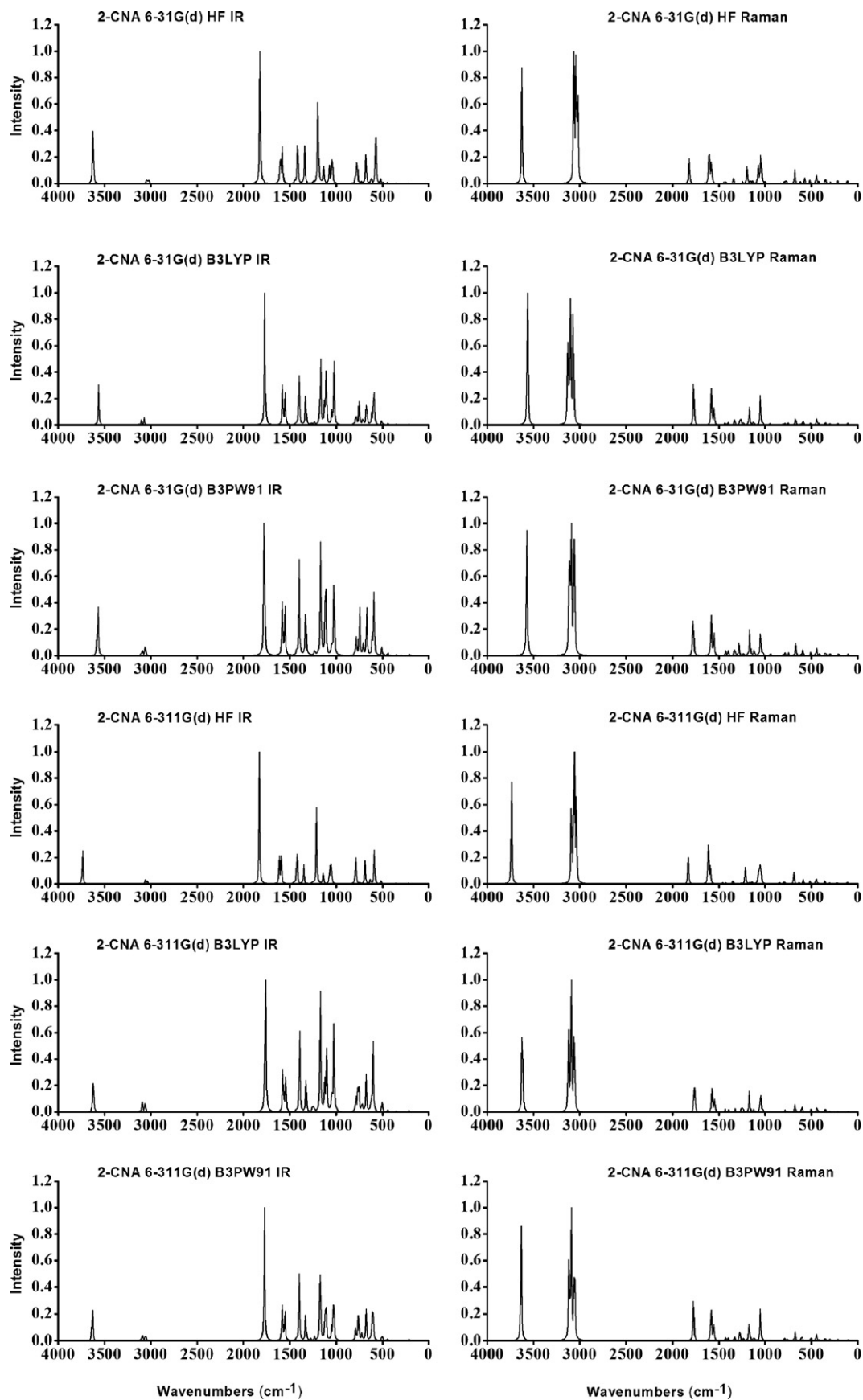


Fig. 3. Comparison of calculated frequencies in  $\text{cm}^{-1}$  normalized IR and Raman intensities at each level of theory considered for 2-CNA.



region (Table 2). Among the calculated fundamentals, the best agreements between experimental and calculated intensities are in high frequency region ( $\sim 3000\text{--}3200\text{ cm}^{-1}$ ). While experimental and calculated high intensities may lead to the true identification in the assignments of fundamentals, theoretical and experimental low intensities may lead to the wrong identification in the assignment of fundamentals [24], especially in the lowest frequency region. As known previously, because of such reasons, i.e. anharmonic effect, vibrational intensity could not be estimated very accurately using quantum chemistry software till now.

To make comparison with experimental data, we present RMS ( $\sigma$ ) values based on the calculations bottom of Table 2. As seen in Table the vibrational frequencies calculated by means of the B3LYP method are the closest to experimental data and B3LYP method correlates well for vibrational frequencies compared with other methods. The best RMS vibrational frequencies values are about 24,508 and 22,984 for 2-CNA with 6-31G(d) and 6-311G(d).

## 5. Conclusion

First time, we have studied experimental and theoretical infrared and Raman spectra of title compound (2-CNA). We have calculated the geometric parameters and vibrational frequencies of 2-CNA molecule by using B3LYP, B3PW91 and HF methods with 6-31G(d) and 6-311G(d). The optimized geometric parameters (bond lengths and bond angles) obtained by using HF show the best agreement with the experimental values of 2-CNA. Comparison of the observed fundamental vibrational frequencies of 2-CNA and calculated results by density functional (B3LYP and B3PW91) and HF method indicate that B3LYP is superior to the scaled HF and B3PW91 approach for molecular vibrational problems. On the basis of the calculated and experimental results, assignment of the fundamental vibrational frequencies has been examined.

## Acknowledgement

This work was supported by the Scientific Research fund of Afyonkarahisar Kocatepe University. Project No. 051.FENED.07.

## References

- [1] S. Gao, J. Liu, L. Huo, Z. Sun, J. Gao, S. Weng Ng, *Acta Cryst.* (2004) m363–m365.
- [2] W.B. Wright, G.S.D. King, *Acta Cryst.* 6 (1953) 305–317.
- [3] A. Kutoglu, C. Scherlinger, *Acta Cryst.* C39 (1983) 232–234.
- [4] N.K. Singh, D.K. Singh, et al., *Synth. React. Inorg. Met.-Org. Chem.* 32 (2002) 203.
- [5] P. Koczon, J.Cz. Dobrowolski, W. Lewandowski, A.P. Mazurek, *J. Mol. Struct.* 655 (2003) 89–95.
- [6] O. Sala, N.S. Gonçalves, L.K. Noda, *J. Mol. Struct.* 565–566 (2001) 411–416.
- [7] W.C.J. Ross, *Biochem. Pharmacol.* 16 (1967) 675–680.
- [8] S.Y. Lee, B.H. Boo, *Bull. Korean Chem. Soc.* 17 (1996) 760.
- [9] S.Y. Lee, B.H. Boo, *Bull. Korean Chem. Soc.* 17 (1996) 754.
- [10] F.J. Devlin, J.W. Finley, P.J. Stephens, M.J. Frish, *J. Phys. Chem.* 99 (1995) 16883.
- [11] N.C. Handy, C.W. Murray, R.D. Amos, *J. Phys. Chem.* 97 (1993) 4392.
- [12] N.C. Handy, P.E. Maslen, R.D. Amos, J.S. Andrews, C.W. Murray, G. Laming, *Chem. Phys. Lett.* 197 (1992) 506.
- [13] N. Sundaraganesan, S. Ilakiamani, H. Saleem, P.M. Wojciechowski, D. Michalska, *Spectrochim. Acta A* 61 (2005) 2995.
- [14] G. Rauhut, P. Pulay, *J. Phys. Chem.* 99 (1995) 3093.
- [15] M.J. Frisch, G.W. Trucks, H.B. Schlegel, G.E. Scuseria, M.A. Robb, J.R. Cheeseman, V.G. Zakrzewski, J.A. Montgomery, Jr., R.E. Stratmann, J.C. Burant, S. Dapprich, J.M. Millam, A.D. Daniels, K. N. Kudin, M.C. Strain, O. Farkas, J. Tomasi, V. Barone, M. Cossi, R. Cammi, B. Mennucci, C. Pomelli, C. Adamo, S. Clifford, J. Ochterski, G.A. Petersson, P.Y. Ayala, Q. Cui, K. Morokuma, D.K. Malick, A.D. Rabuck, K. Raghavachari, J.B. Foresman, J. Cioslowski, J.V. Ortiz, A.G. Baboul, B.B. Stefanov, G. Liu, A. Liashenko, P. Piskorz, I. Komaromi, R. Gomperts, R.L. Martin, D.J. Fox, T. Keith, M.A. Al-Laham, C.Y. Peng, A. Nanayakkara, M. Challacombe, P.M.W. Gill, B. Johnson, W. Chen, M.W. Wong, J.L. Andres, C. Gonzalez, M. Head-Gordon, E.S. Replogle, J.A. Pople, *GAUSSIAN 03*, Revision A.9, Gaussian, Inc., Pittsburgh, PA, 2003.
- [16] M.V.N. de Souza, S.M.S.V. Wardell, R.A. Howie, *Acta Cryst.* E61 (2005) o1347–o1349.
- [17] S.H. Vosko, L. Wilk, M. Nusair, *Can. J. Phys.* 58 (1980) 1200.
- [18] P.L. Fast, J. Corchado, M.L. Sanches, D.G. Truhlar, *J. Phys. Chem. A* 103 (1999) 3139.
- [19] NIST Chemistry Webbook, IR database, <http://srdata.nist.gov/cccbdb>.
- [20] A. Frisch, A.B. Nielsen, A.J. Holder, *Gaussview Users Manual*, Gaussian Inc., Pittsburg.
- [21] N. Sundaraganesan, B.D. Joshua, K. Settu, *Spectrochim. Acta A* 66 (2007) 381–388.
- [22] M. Kurt, Ş. Yurdakul, *J. Mol. Struct.* 654 (2003) 1–9.
- [23] J.O. Jensen, *Vib. Spectrosc.* 30 (2002) 191.
- [24] J.E. del Bene, *J. Am. Chem. Soc.* 101 (1979) 6184.
- [25] G. Fischer, P. Wormel, *Chem. Phys.* 198 (1995) 183.
- [26] M. Kurt, Ş. Yurdakul, *J. Mol. Struct.: Theochem* 730 (2005) 59–67.
- [27] B.G. Johnson, P.M. Gill, J.A. Pople, *J. Chem. Phys.* 98 (1993) 5612.
- [28] M. Bakiler, I.V. Maslov, S. Akyüz, *J. Mol. Struct.* 482–483 (1998) 379.
- [29] M. Bakiler, I.V. Maslov, S. Akyüz, *J. Mol. Struct.* 475 (1999) 83.
- [30] M. Kurt, M. Yurdakul, Ş. Yurdakul, *J. Mol. Struct.* 711 (2004) 25–32.
- [31] A.K. Rai, S. Kumar, A. Rai, *Vib. Spectrosc.* 42 (2006) 397.
- [32] A.E. Ozel, S. Kecel, S. Akyüz, *Vib. Spectrosc.* 42 (2006) 325.
- [33] L. Santos, E. Martinez, B. Ballesteros, J. Sanchez, *Spectrochim. Acta Part A* 56 (2000) 1905.
- [34] J. Hanuza, M. Maczka, A. Waslowska, W. Oganowski, M. Andruszkiewicz, H.B. Ogonowska, B. Lutz, V. der-Maas, *J. Mol. Struct.* 404 (1997) 33.